



Differential induction of apoptosis in demyelinating and nondemyelinating infection by mouse hepatitis virus

Talya Schwartz, Li Fu, and Ehud Lavi

Department of Pathology and Laboratory Medicine, Division of Neuropathology, University of Pennsylvania, School of Medicine, Philadelphia, Pennsylvania, USA

The role of apoptosis in mouse hepatitis virus (MHV) infection is still controversial. To better assess the role of apoptosis in MHV infection, we used three different biologic phenotypes of MHV to examine their differential effect on the induction of apoptosis. MHV-A59 produces acute hepatitis, meningoencephalitis, and chronic demyelination. MHV-2 causes only acute hepatitis and meningitis, whereas Penn98-1 produces acute hepatitis and meningoencephalitis without demyelination. We detected TdT-mediated dUTP nick-end labeling (TUNEL) staining in the livers and meninges of MHV-A59-, MHV-2-, and Penn98-1-infected mice. TUNEL staining in brain parenchyma was only detected in MHV-A59- and Penn98-1-infected mice. We detected apoptosis by electron microscopy in olfactory neurons during acute infection with MHV-A59. The kinetics and distribution of TUNEL staining correlated with the pathologic damage and colocalized with viral antigen in some cells. At 1 month, TUNEL staining was found exclusively in areas of demyelination in the spinal cord of MHV-A59-infected mice; however, it was not found in nondemyelinated mice infected with MHV-2 or Penn98-1, or in mock-infected mice. TUNEL-positive cells were identified as macrophage/microglial cells, some astrocytes, and some oligodendrocytes, by colabeling with cell-specific markers. The presence of TUNEL staining in oligodendrocytes suggests that apoptosis may play an important role in MHV-induced demyelination. *Journal of NeuroVirology* (2002) 8, 392–399.

Keywords: apoptosis; coronaviruses; demyelination; mouse hepatitis virus; multiple sclerosis; Nidovirales

Address correspondence to Dr. Ehud Lavi, University of Pennsylvania, School of Medicine, Division of Neuropathology, Department of Pathology and Laboratory Medicine, 613 Stellar-Chance Laboratories, 422 Curie Boulevard, Philadelphia, PA 19104-6100, USA. E-mail: lavi@mail.med.upenn.edu

Portions of this work were presented at the meeting “Programmed Cell Death Regulation: Basic Mechanisms and Therapy” in Lake Tahoe, Nevada, March, 2000, and at the VIIth International Symposium on Nidoviruses, May, 2001, Lake Harmony, Pennsylvania. The authors thank Donna Bauhof for critical review of the manuscript, Elsa Aglow and Neelima Shah for excellent histology and EM expertise. This work was supported in part by a grant from the National Multiple Sclerosis Society (RG 2615) and a PHS grant NS30606.

Received 18 March 2002; revised 10 June 2002; accepted 1 July 2002.

Introduction

Mouse hepatitis viruses (MHV) are a group of hepatoencephalitic coronaviruses, of the Nidovirales order, which are common natural pathogens in mice (Lai and Cavanagh, 1997; Lavi and Weiss, 1989). MHV-A59 is a neurotropic virus that causes a biphasic disease in susceptible mice. Acute disease consists of severe hepatitis and focal meningoencephalitis, whereas chronic disease consists of demyelinating lesions, found mainly in the spinal cord (Lavi *et al.*, 1984b). The resemblance to multiple sclerosis (MS) makes it an attractive experimental model for MS (Lavi *et al.*, 1984a; Lavi *et al.*, 1999). MHV-2,

on the other hand, causes a monophasic disease, consisting of acute hepatitis and meningitis (Das Sarma *et al*, 2001b). Penn98-1 is a recombinant virus produced with the backbone of MHV-A59 and an S gene derived from MHV-2. It causes acute hepatitis and meningoencephalitis but does not cause demyelination (Das Sarma *et al*, 2000). The phenotypic difference between these three closely related viruses provides an opportunity to study the contribution of various phenotypic properties to pathogenesis.

Apoptosis has been reported following various viral infections (Razvi and Welsh, 1995). Apoptosis induces elimination of virus-infected cells by cytotoxic T cells (Shibata *et al*, 1994); it slows viral spread (Clem *et al*, 1991), or participates in an autoimmune process (Osborne, 1996). Sindbis virus infection causes apoptosis during fatal encephalomyelitis in neonatal mice, whereas infection of adult mouse brain results in insignificant cytopathology and only minimal apoptosis (Griffin *et al*, 1994a, 1994b). Theiler's murine encephalomyelitis virus (TMEV) infection is associated with abundant apoptosis in neurons and in mononuclear cells in the brain and spinal cord during acute infection. During the chronic demyelinating disease induced by the virus, apoptotic oligodendrocytes, macrophages, microglia, and astrocytes are found in demyelinating lesions (Palma *et al*, 1999; Tsunoda *et al*, 1997). In experimental allergic encephalomyelitis (EAE), the disease is much milder in mice lacking Fas and Fas ligand molecules, with equal inflammatory response, suggesting that apoptosis contributes to the clinical disease and demyelination (Okuda *et al*, 1998; Sabelko *et al*, 1997; Waldner *et al*, 1997). A pan-caspase inhibitor, injected prior to immunization, significantly reduces the incidence of EAE. Treated animals show less inflammatory infiltrates and demyelination, and reduced axonal loss (Furlan *et al*, 1999). However, though molecules of the apoptotic cascade are well represented in the central nervous system (CNS) during the disease process in EAE, their expression is mainly in inflammatory cells and microglia but not in oligodendrocytes (Bonetti and Raine, 1997).

The role of apoptosis in MHV-induced disease is still under debate. Two studies show apoptotic T cells, macrophages, astrocytes, and oligodendrocytes in MHV-(JHM) infection (Barac-Latas *et al*, 1997; Wu and Perlman, 1999), but neither one of these studies compared demyelinating viruses with nondemyelinating viruses, and therefore were unable to directly address the relevance of apoptosis to demyelination. In one of these reports, the authors interpreted the finding as indicating that the distribution of demyelination correlates with macrophage infiltration better than with the presence of apoptotic cells (Wu and Perlman, 1999). This study did not investigate the nature of the apoptotic cells by cell-specific markers and therefore could not identify parenchymal cell apoptosis. In another study, Fas-deficient mice infected with JHM virus variant

J2.2-v1 did not show a different level of demyelination and inflammation from wild-type infected mice (Parra *et al*, 2000). However, apoptosis can occur by a Fas-independent mechanism. In the present study we re-examined the potential role of apoptosis in MHV-induced disease using a variety of MHV strains with different biologic properties. We used a demyelinating strain of the virus (MHV-A59) in comparison to a nondemyelinating, strain (MHV-2), which we recently sequenced and characterized (Das Sarma *et al*, 2001b), and two newly constructed recombinant viruses (Penn98-1 and Penn98-2) that present a hybrid phenotype (Das Sarma *et al*, 2000). The availability of these closely related viruses that differ in the demyelination phenotype helps to better define the role of apoptosis in demyelination.

Results

Acute stage—apoptosis was found in areas of pathologic damage

TdT-mediated dUTP nick-end labeling (TUNEL) staining was detected in the brains and livers of mice infected with MHV-A59, Penn98-1, and MHV-2. Extensive apoptosis was found in the liver in all types of infections, and was strictly associated with areas of necrosis and inflammation, representing hepatitis. The difference in the distribution pattern of apoptosis correlated with the difference in the extent of hepatitis present in these three viral infections. MHV-A59 infection caused distinctive foci of hepatitis and apoptosis (Figure 1A), whereas MHV-2 and Penn98-1 caused an extensively disseminated pattern (Navas *et al*, 2001). TUNEL-positive nuclei were detected as early as 1 day post infection with MHV-2, whereas apoptotic cells in MHV-A59 infection were detected only after 3 days post infection. Apoptotic staining peaked at 5 to 7 days post infection but was no longer detectable 11 days post infection (Figure 2A). Rare cells, identified morphologically as hepatocytes, exhibited double staining with TUNEL and MHV antigen (Figure 1F). The distribution of TUNEL-positive cells in the liver was similar to the distribution of MHV-infected cells. The disseminated pattern induced by MHV-2 and Penn98-1 in the liver correlated with antigen distribution.

Apoptosis in the meninges was found in mice infected with MHV-A59, Penn98-1, or MHV-2. TUNEL-positive cells were detected from 1 day post infection in MHV-2-infected mice and 3 days post infection in MHV-A59-infected mice, and were observed until 8 days post infection. Positive cells were more abundant in MHV-2-infected mice (level 3) (Figure 1E), compared with MHV-A59-infected mice (level 2). Labeling was also seen in some ependymal and subependymal cells.

Brain parenchymal apoptosis correlated with the degree of encephalitis and was found mainly in

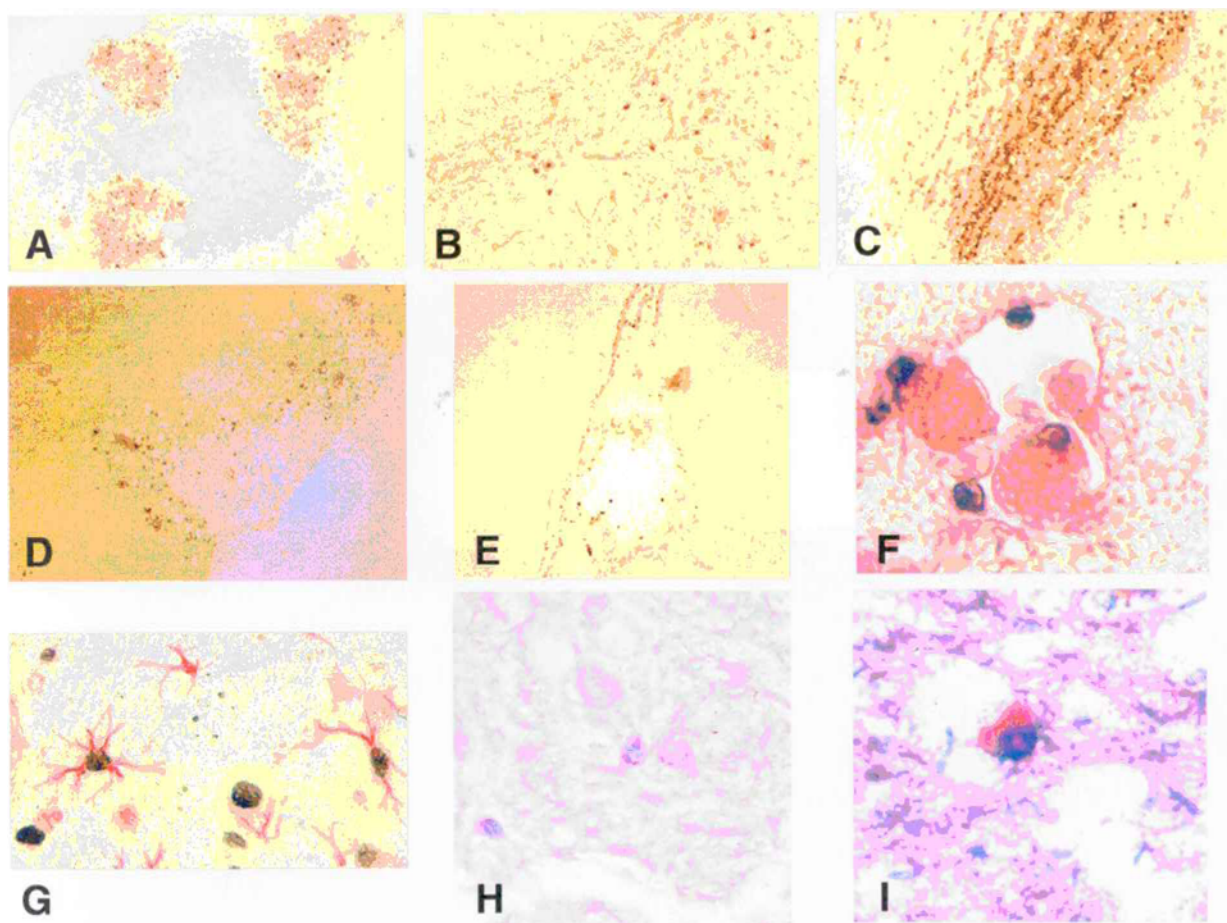


Figure 1 (A) TUNEL staining of a mouse liver section 5 days after IC infection with MHV-A59. Note focal positive signal in multiple cells, associated with foci of hepatitis (100 \times). (B) TUNEL staining of a mouse brain section 5 days after IC infection with MHV-A59. Note scattered positive signal in areas of acute encephalitis (100 \times). (C) TUNEL staining in the olfactory bulb of a mouse 5 days after IC infection with MHV-A59. The olfactory bulb was the area of most extensive TUNEL signal during acute infection (100 \times). (D) TUNEL staining of a spinal cord 30 days after IC infection with MHV-A59. A demyelinating lesion is seen at the anterior column of the cord's white matter, shown here as less intense brown staining. Note positive TUNEL signal at the periphery of the demyelinating lesion, but very little in other parts of the white matter (100 \times). (E) TUNEL staining of a mouse brain section 5 days after IC infection with MHV-2. Note positive TUNEL signal restricted to the meninges, and occasional subpial cells (100 \times). (F) Liver section from a mouse 5 days following IC infection with MHV-A59. TUNEL staining (black) combined with immunohistochemistry, was applied using anti-MHV rabbit polyclonal antibodies (red). Note viral antigen in TUNEL-positive hepatocytes (400 \times). (G) Spinal cord section from a mouse 30 days after IC infection with MHV-A59. TUNEL staining (black) was combined with immunohistochemistry (red) using anti-GFAP antibodies. Next to a demyelinating area, note two GFAP-positive cells (astrocytes) also expressing TUNEL staining (400 \times). (H) Spinal cord section from a mouse 30 days after IC infection with MHV-A59. TUNEL staining (blue) was combined with immunohistochemistry (red) using anti-CAII antibodies. Close to a demyelinating area note at the center a CAII-positive cell (oligodendrocyte) also expressing TUNEL staining next to a CAII-positive, TUNEL-negative oligodendrocyte. Another TUNEL-positive oligodendrocyte is also present (400 \times). (I) Spinal cord section from a mouse 30 days after IC infection with MHV-A59. TUNEL staining (black) was combined with immunohistochemistry (red) using F4/80 antibodies. Next to a demyelinating lesion note an F4/80-positive cell (macrophage/microglia) also expressing TUNEL staining (400 \times).

MHV-A59– and, to a lesser extent, in Penn98-1–infected mice. There was no brain parenchymal TUNEL staining, and no encephalitis, in MHV-2–infected brains. The distribution of TUNEL-positive cells in MHV-A59–infected mice was predominantly in the olfactory bulb, basal forebrain, subiculum, entorhinal cortex, thalamus, hypothalamus, amygdala, and corpus callosum (Figure 1B, C). The distribution correlated with the distribution of pathology and viral antigen as previously described (Lavi *et al.*, 1988). Only rare cells expressed both

viral antigen and TUNEL labeling in the brain of MHV-A59– and Penn98-1–infected mice, and rare cells expressed both TUNEL and viral antigen in the meninges of MHV-2–infected mice. The vast majority of the TUNEL-positive cells were antigen negative and many antigen-positive cells were TUNEL negative. Apoptosis was noticed from day 3 post infection, peaked on day 5 (level 3), and was no longer detectable on day 11 (Figure 2B). In all the kinetics studies of apoptosis, there was only minimal differences between mice of the same time point.

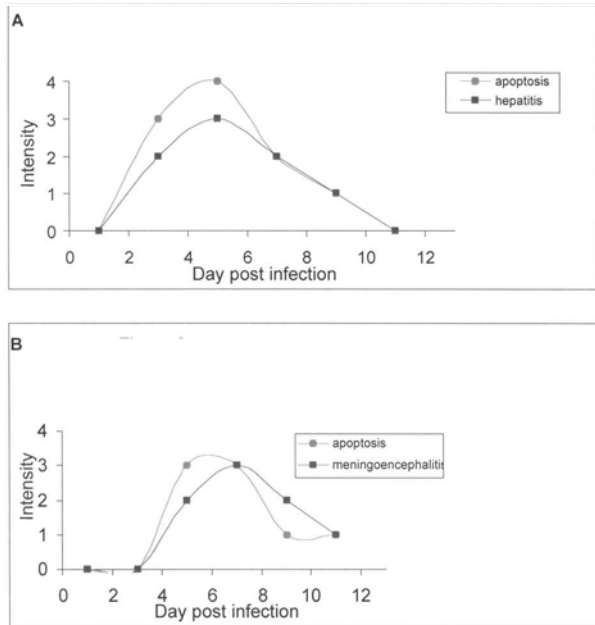


Figure 2 A, Kinetics of apoptosis and hepatitis during the acute phase following IC infection with MHV-A59. The intensity of apoptosis and hepatitis was determined as described in the text. B, Kinetics of apoptosis and meningoencephalitis during the acute phase following IC infection with MHV-A59. The intensity of apoptosis and hepatitis was determined as described in the text.

Mock-infected mice with L2 lysate had negative TUNEL staining in all tissues.

The presence of apoptosis in the olfactory bulb was also investigated by electron microscopy and compared with TUNEL staining. Following intranasal infection, the olfactory bulbs had the highest concentration of TUNEL-positive cells at 5 days post infection. Electron microscopy (EM) analysis of the olfactory bulb of two MHV-A59-infected mice revealed numerous neurons showing condensation of nuclei and fragmentation of the chromatin, characteristic of apoptosis, whereas the olfactory bulb of a mock-infected control mouse showed normal morphology without any evidence of apoptosis (Figure 3).

Chronic stage—apoptosis was found in areas of demyelination

TUNEL staining was observed in the spinal cords obtained 30 days post infection exclusively in demyelination-positive mice (infected with 5 or 25 PFU of MHV-A59). Seven out of 10 mice infected with 5 PFU A59 and 8 of 8 mice infected with 25 PFU A59 developed demyelination. All 15 demyelination-positive mice were TUNEL positive. Three demyelination-negative mice infected with 5 PFU A59 did not stain for apoptosis. Apoptotic cells were detected mainly in the white matter at the edges of the demyelinating lesions (Figure 1D), though some cells were also seen in the gray matter. Demyelination and apoptosis were not detected in the

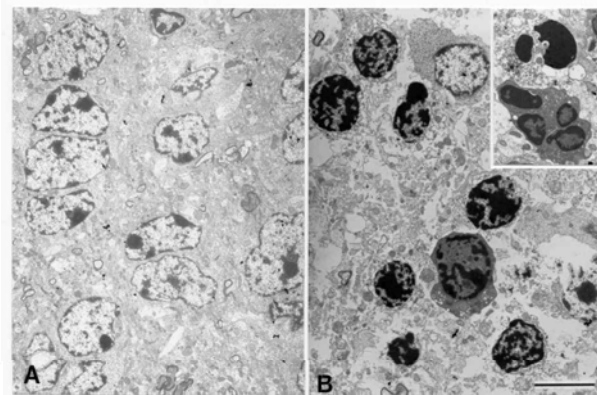


Figure 3 Electron micrographs of olfactory bulbs of mice 5 days after intranasal inoculation of (A) L2 cell lysate (control) or (B) MHV-A59. Normal olfactory neurons are seen following sham-injection, whereas the MHV-A59 infected mouse showed numerous olfactory neurons with chromatin condensation and/or fragmentation, consistent with a morphological picture of apoptosis. The insert shows additional apoptotic nuclei with fragmentation and condensation of chromatin in a different field. The bar represents 5 microns.

spinal cords of 28 of 28 infected mice with 5 PFU of MHV-2 or 50 PFU of MHV-2 (18 and 10 mice, respectively). Only rare positive TUNEL staining was seen in 3 of 14 mice infected with 5 PFU of Penn98-1 and Penn98-2. There was no demyelination detected in Penn98-1- and Penn98-2-infected mice (0 of 14). TUNEL staining was not found in 10 of 10 mock-infected control mice. During the chronic stage, TUNEL staining was negative in the brain parenchyma and liver of all MHV-2- or MHV-A59-infected mice.

Identification of cell type of cells undergoing apoptosis

To assess the nature of the apoptotic cells during chronic demyelinating infection, we performed double labeling for TUNEL-positive nuclei and immunohistochemical staining for specific markers of astrocytes, oligodendrocytes, and macrophages/microglial cells. TUNEL-positive cells were identified as macrophages/microglial cells, oligodendrocytes, and astrocytes. A few cells, morphologically consistent with lymphocytes, also appeared to be TUNEL positive. Quantification studies of the TUNEL-positive cells demonstrated 3% to 5% CAII-positive cells (Figure 1H), 1% to 2% glial fibrillary acidic protein (GFAP)-positive cells (Figure 1G), and 70% of the cells were double stained with F4/80 (a mouse microglial/macrophage marker) (Figure 1I) out of all TUNEL-positive stained cells. The oligodendrocytic markers including CAII, (MBP), or cNase are notoriously weaker than GFAP on formalin-fixed tissue. In order to be able to detect double staining in oligodendrocytes, the concentration of the TUNEL signal had to be decreased. Nevertheless, we clearly detected TUNEL-positive labeling in CAII (Figure 1H) and cNase (not shown)-positive oligodendrocytes.

Discussion

In this study we evaluate the effect of apoptosis on the acute and the chronic stages of MHV-induced disease in mice. We use different strains and recombinant viruses with various biologic phenotypes to assess the contribution of apoptosis to the different components of the pathologic process, especially demyelination. Having the advantage of the different biologic phenotypes of the virus, we are able to show for the first time that apoptosis correlates with the pathologic damage in MHV infection. During acute infection, apoptosis is found in the livers of all three viral phenotypes, as all three viruses cause hepatitis. TUNEL-positive cells are also seen in acute encephalitis; however, the intensity of staining does not always correlate with the intensity of the pathologic process. Whereas acute encephalitis in MHV-A59 infection is associated with extensive TUNEL-positive cells, the encephalitis caused by Penn98-1 and Penn98-2 is not accompanied by extensive TUNEL staining. We have previously shown that acute encephalitis caused by Penn98-1 and Penn98-2 is similar to MHV-A59-induced encephalitis in viral titers, inflammatory infiltration, and viral antigen distribution (Das Sarma *et al*, 2000). The reduced ability of the Penn98 viruses to cause apoptosis may be an inherent property of these viruses, unrelated to CNS viral load. TUNEL staining was not detected in brain parenchyma of MHV-2-infected mice, consistent with a lack of brain parenchymal involvement in MHV infection (Das Sarma *et al*, 2001b).

Apoptosis in MHV infection occurs in both inflammatory and parenchymal cells. Morphological identification of apoptosis in hepatocytes in the liver and in neurons in the olfactory bulb supports the hypothesis that at least some of the parenchymal cell death during acute infection is due to apoptosis. Apoptotic cells are prevalent in regions of high viral titers (Fishman *et al*, 1985; Lavi *et al*, 1988), but colabeling of TUNEL and viral antigen was seen only in a few cells in brain and liver. Also, TUNEL staining is not present in all dying cells, suggesting that apoptosis is not an exclusive path of cell death in this infection, and that a significant number of cells were also undergoing necrosis. The virus may induce apoptosis directly in infected cells or indirectly in uninfected cells by mediator molecules such as tumor necrosis factor (TNF) secreted by infected cells. An *et al* (1999) showed that MHV-A59 causes apoptosis in vitro in 17CL-1 cells, but not in DBT cells, in spite of productive infection in both cell lines; this indicates that apoptosis is not a universal mechanism of cell death in MHV infection.

During the chronic stage of disease, TUNEL-positive cells correlate very well with the demyelinating lesions in the spinal cord. Only demyelinated mice infected with MHV-A59 exhibit a significant amount of TUNEL-positive staining during the chronic stage of disease. There is no

significant amount of TUNEL staining in any of the demyelination-negative mice infected with MHV-2, Penn98-1, or Penn98-2. This may suggest that apoptosis plays an active role in the process of demyelination in MHV infection. Additional studies are necessary to determine whether the site of molecular determinants of apoptosis is in the S gene as it has been shown for other biologic properties of the virus (Das Sarma *et al*, 2000, 2001a; Navas *et al*, 2001).

Among the TUNEL-positive cells during demyelination, macrophages/microglial cells represented the majority of the TUNEL-positive cells. Proliferating macrophages and microglial cells play a very important role in the demyelinating process and apoptosis may be a mechanism of controlling the number of these cells in areas of damage. The distribution of F4/80+ cells is found to be mainly in the center of the demyelinated lesion, as has been shown in other experimental systems of demyelination. Their role in demyelination is still debated, because these cells may have both functions that may indicate active role in demyelination or just as phagocytic elements to collect the myelin and cellular debris from the lesion. Similar role may be attributed to the apoptosis found in a small number of astrocytes near areas of damage. Apoptosis may represent a mechanism of controlling the level of proliferating astrocytes in reactive gliosis. However, TUNEL staining is also detected in CAII-positive oligodendrocytes. Because TUNEL staining usually indicates an irreversible stage in the life of a cell, the presence of apoptosis in oligodendrocytes suggests that at least part of the demyelinating process is due to programmed cell death in oligodendrocytes. In the CNS, a single oligodendrocyte is responsible for the myelination of a large number of axons. The loss of only very few oligodendrocytes can account for extensive demyelinating damage. Moreover, apoptosis is usually a fast event and fragments of apoptotic cells are quickly phagocytosed (Majno and Joris, 1995) and only a small amount of ongoing active demyelination can be detected at any given time point. Thus, we conclude that, even if only a small number of oligodendrocytes in areas adjacent to the areas of demyelination are detected containing TUNEL staining at any particular time point in MHV infection, apoptosis is nevertheless a significant factor in MHV-induced demyelination. The fact that the majority of the apoptotic cells were macrophages and lymphocytes, as also reported in JHM infection (Wu and Perlman, 1999), should not diminish the importance of apoptotic parenchymal cells.

Apoptosis has been observed in a wide variety of neurological diseases and in various viral infections. Apoptosis in oligodendrocytes was also reported following Theiler's virus infection (Tsunoda *et al*, 1997). The role of apoptosis in the pathogenesis of MS is not completely clear. Apoptosis is observed in association with demyelinating lesions in patients with MS, and up to 40% of apoptotic cells in postmortem chronic MS lesions are identified as oligodendrocytes

(Dowling *et al*, 1997). Up-regulation of Fas antigen on oligodendrocytes (Bonetti *et al*, 1997) and increase of the soluble form of the antigen in the cerebrospinal fluid (CSF) and the serum of patients were also reported (Giusani *et al*, 1998; Zipp *et al*, 1998). On the other hand, expression of Fas was reported on oligodendrocytes, and oligodendrocytes death was presumed to be associated with this expression, but without evidence of apoptosis (D'Souza *et al*, 1996). Others do not find a difference in Fas soluble levels in the serum between patients with MS and controls (Bansil *et al*, 1997).

Apoptotic inflammatory cells, resident target cells, and apoptotic molecules are detected in the CNS in the three main experimental animal models of demyelination: TMEV, EAE, and MHV. However, no conclusions have been reached regarding the direct role of apoptosis in the demyelinating process. Barac-Latas *et al* (1997) demonstrate both apoptotic and necrotic oligodendrocytes following MHV-JHM infection, and Tsunoda and Fujinami (1996) detect oligodendrocytes apoptosis in EAE and TMEV, whereas Bonetti shows up-regulation of Fas molecules on oligodendrocytes in EAE, which were found abundantly in the CD3+ cells undergoing apoptosis, but finds no other features of apoptosis (Bonetti and Raine, 1997).

In conclusion, apoptosis may play an important role in both acute and chronic MHV disease, most significantly in demyelination. The small number of the apoptotic cells, and the distribution of these cells at the periphery of the demyelinating lesion, are consistent with the nature of the demyelinating process. The relationship between apoptosis, inflammation, and tissue damage needs further investigation, perhaps by further dissection of the apoptotic cascade.

Materials and methods

Viruses

MHV-A59 (Budzilowicz *et al*, 1985; Lavi *et al*, 1984b), MHV-2 (Keck *et al*, 1988), and Penn98-1 and Penn98-2 (Das Sarma *et al*, 2000) were used in this study. Viruses were grown and viral titers were determined on L2 cells by standard plaque assays (Lavi *et al*, 1984b).

Mice

Pathogen-free, 4-week-old male C57BL/6 mice were obtained from the Jackson Laboratory (Bar Harbor, ME). Mice were injected intracerebrally (IC) with 2.5×10^3 , 25, and 5 plaque-forming units (PFU) of MHV-A59; 50 and 5 PFU of MHV-2, Penn98-1, or Penn98-2. Mock-infected mice were injected IC with L2 cell lysate. For electron microscopy analysis, mice were infected intranasally (IN) with 5×10^9 PFU/ml of MHV-A59 or mock-infected intranasally with cell lysate. The IN injection increased the concentration of infected cells in the olfactory bulbs and therefore

was ideal for EM studies. As we have previously shown, the disease process in IC and IN inoculations is similar (Lavi *et al*, 1984b, 1986, 1988).

Histology

Mice were sacrificed on days 1, 3, 5, 7, 9, 11, 30 (two to three mice per time point per virus during the acute stage and 53 mice on day 30). All mice were perfused transcardially with phosphate-buffered saline. Brain, spinal cord, and liver were removed and fixed in 10% normal-buffered formalin at room temperature for 48 h, embedded in paraffin, and sectioned into 5 μ m. For examination of demyelination and inflammation, sections were stained with luxol fast blue (LFB) and hematoxylin and eosin, respectively.

The intensity of hepatitis was evaluated based on the following criteria: 0, no lesions are detected; 1, rare (one or two) necrotic inflammatory lesions are detected in each liver section; 2, several (three to five) necrotic lesions are identified in each liver section; 3, severe hepatitis consisting of more than five separate lesions in each section; 4, confluent liver damage with bridging hepatitis lesions throughout each section. The intensity of encephalitis was evaluated in the following manner: 0, no lesions; 1, rare focal perivascular inflammatory infiltrates; 2, mild multifocal inflammatory infiltrates and microglial proliferation; 3, severe multifocal encephalitis; 4, panencephalitis involving every region of the brain.

TUNEL

Detection of *in situ* DNA fragmentation was done with fluorescein *in situ* cell death detection kit (Boehringer Mannheim, Indianapolis, IN) as specified by the manufacturer. Quantitative intensity of apoptotic staining was divided into 4 levels: 1, mild (20–100 cells/section); 2, moderate (100–200 cells/section); 3, severe (200–350 cells/section); 4, extremely severe (>350 cells/section).

Double labeling

Double labeling was performed with TUNEL and MHV antibodies or cell-specific markers. After completion of TUNEL staining using nitroblue tetrazolium (NBT)/5-bromo-4-chloro 3-indolyl phosphate (BCIP) as a staining substrate, a 1:200 dilution of rabbit anti-MHV-A59 polyclonal antibody and 1:100 dilution of monoclonal GFAP (Lee *et al*, 1984) were applied for 2 h at 37°C, respectively. Immunohistochemical staining was done by the UltraProbe kit (Biomedica, Foster City, CA), applying secondary biotinylated antibody for 15 min at 37°C, followed by the avidin-phosphatase reagent for 15 min at 37°C. Fast-red (Biomedica) was used as the staining substrate. Double labeling for oligodendrocytes or macrophage specific markers was done as follows. Sections were permeabilized with 0.1% Triton X-100, then incubated with carbonic anhydrase II (1:500 dilution) (Cammer *et al*, 1985), or rat anti-mouse F4/80 antigen (1:500, Serotec, Raleigh, NC) for 2 h at 37°C. Immunohistochemical staining was then done as

described above with Vector blue (Vector laboratories, Burlingame, CA) as the staining substrate. After the completion of the immunohistochemical staining, we applied the TUNEL reaction, using Fast-red (Biomeda) as the staining substrate. Negative controls included the omission of the primary antibodies, the omission of the TUNEL labeling mixture, or the application of primary irrelevant antibodies at the same concentration. We evaluated labeling by light microscopy, and the quantification of double staining was expressed as the number of positive double-stained cells per section. Two to three sections were evaluated for each one of the antibodies.

References

- An S, Chen CJ, Yu X, Leibowitz JL, Makino S (1999). Induction of apoptosis in murine coronavirus-infected cultured cells and demonstration of E protein as an apoptosis inducer. *J Virol* **73**: 7853–7859.
- Bansil S, Holtz CR, Cook SD, Rohowsky-Kochan C (1997). Serum sAPO-1/Fas levels in multiple sclerosis. *Acta Neurol Scand* **95**: 208–210.
- Barac-Latas V, Suchanek G, Breitschopf H, Stuehler A, Wege H, Lassmann H (1997). Patterns of oligodendrocyte pathology in coronavirus-induced subacute demyelinating encephalomyelitis in the Lewis rat. *Glia* **19**: 1–12.
- Bonetti B, Pohl J, Gao YL, Raine CS (1997). Cell death during autoimmune demyelination: Effector but not target cells are eliminated by apoptosis. *J Immunol* **159**: 5733–5741.
- Bonetti B, Raine CS (1997). Multiple sclerosis: Oligodendrocytes display cell death-related molecules in situ but do not undergo apoptosis. *Ann Neurol* **42**: 74–84.
- Budzilowicz CJ, Wilczynski SP, Weiss SR (1985). Three intergenic regions of mouse hepatitis virus strain A59 genome RNA contain a common nucleotide sequence that is homologous to the 3' end of the viral mRNA leader sequence. *J Virol* **53**: 834–840.
- Cammer W, Sacchi R, Sapirstein V (1985). Immunocytochemical localization of carbonic anhydrase in the spinal cords of normal and mutant (shiverer) adult mice with comparisons among fixation methods. *J Histochem Cytochem* **33**: 45–54.
- Ciusani E, Frigerio S, Gelati M, Corsini E, Dufour A, Nespolo A, La Mantia L, Milanese C, Massa G, Salmaggi A (1998). Soluble Fas (Apo-1) levels in cerebrospinal fluid of multiple sclerosis patients. *J Neuroimmunol* **82**: 5–12.
- Clem RJ, Fechheimer M, Miller LK (1991). Prevention of apoptosis by a baculovirus gene during infection of insect cells. *Science* **254**: 1388–1390.
- Das Sarma J, Fu L, Hingley ST, Lai MM, Lavi E (2001a). Sequence analysis of the S gene of recombinant MHV-2/A59 coronaviruses reveals three candidate mutations associated with demyelination and hepatitis. *J Neuro-Viro* **7**: 432–436.
- Das Sarma J, Fu L, Hingley ST, Lavi E (2001b). Mouse hepatitis virus type-2 infection in mice: An experimental model system of acute meningitis and hepatitis. *Exp Mol Pathol* **71**: 1–12.
- Das Sarma J, Fu L, Tsai JC, Weiss SR, Lavi E (2000). Demyelination determinants map to the spike glycoprotein gene of coronavirus mouse hepatitis virus. *J Virol* **74**: 9206–9213.
- Dowling P, Husar W, Menonna J, Donnenfeld H, Cook S, Sidhu M (1997). Cell death and birth in multiple sclerosis brain. *J Neurol Sci* **149**: 1–11.
- D'Souza SD, Bonetti B, Balasingam V, Cashman NR, Barker PA, Troutt AB, Raine CS, Antel JP (1996). Multiple sclerosis: Fas signaling in oligodendrocyte cell death. *J Exp Med* **184**: 2361–2370.
- Fishman PS, Gass JS, Swoveland PT, Lavi E, Highkin MK, Weiss SR (1985). Infection of the basal ganglia by a murine coronavirus. *Science* **229**: 877–879.
- Furlan R, Martino G, Galbiati F, Poliani PL, Smiroldo S, Bergami A, Desina G, Comi G, Flavell R, Su MS, Adorini L (1999). Caspase-1 regulates the inflammatory process leading to autoimmune demyelination. *J Immunol* **163**: 2403–2409.
- Griffin DE, Levine B, Tyor WR, Tucker PC, Hardwick JM (1994a). Age-dependent susceptibility to fatal encephalitis: Alphavirus infection of neurons. *Arch Virol Suppl* **9**: 31–39.
- Griffin DE, Levine B, Ubol S, Hardwick JM (1994b). The effects of alphavirus infection on neurons. *Ann Neurol* **35**: S23–S27.
- Keck JG, Soe LH, Makino S, Stohlman SA, Lai MMC (1988). RNA recombination of murine coronavirus: Recombination between fusion-positive mouse hepatitis virus A59 and fusion-negative mouse hepatitis virus 2. *J Virol* **62**: 1989–1998.
- Lai MMC, Cavanagh D (1997). The molecular biology of coronaviruses. *Adv Virus Res* **48**: 1–100.
- Lavi E, Fishman SP, Highkin MK, Weiss SR (1988). Limbic encephalitis following inhalation of murine coronavirus MHV-A59. *Lab Invest* **58**: 31–36.
- Lavi E, Gilden DH, Highkin MK, Weiss SR (1984a). Persistence of MHV-A59 RNA in a slow virus demyelinating infection in mice as detected by in situ hybridization. *J Virol* **51**: 563–566.
- Lavi E, Gilden DH, Highkin MK, Weiss SR (1986). The organ tropism of mouse hepatitis virus A59 is dependent on dose and route of inoculation. *Lab Anim Sci* **36**: 130–135.
- Lavi E, Gilden DH, Wroblewska Z, Rorke LB, Weiss SR (1984b). Experimental demyelination produced by the A59 strain of mouse hepatitis virus. *Neurology* **34**: 597–603.

Electron microscopy

Three mice were sacrificed 5 days post infection, and olfactory bulbs were collected and fixed in 2.5% glutaraldehyde + 1% paraformaldehyde in 0.1 M cacodylate buffer, pH 7.4 + 0.002% CaCl₂. Tissues were post-fixed in 2% osmium tetroxide, dehydrated in graded ethanol, and, after infiltration with propylene oxide and EPON, were embedded in the same resin. Seventy nanometers thick sections were then stained in uranyl acetate and bismuth subnitrite and viewed by a transmission electron microscope (JEOL JEM1010) at 80 kV as previously described (Lavi *et al*, 1994).

- Lavi E, Schwartz T, Jin YP, Fu L (1999). Nidovirus infections: Experimental model systems of human neurologic diseases. *J Neuropathol Exp Neurol* **58**: 1197–1206.
- Lavi E, Wang Q, Stieber A, Gonatas NK (1994). Polarity of processes with Golgi apparatus in a subpopulation of type I astrocytes. *Brain Res* **647**: 273–285.
- Lavi E, Weiss SR (1989). Coronaviruses. In: *Clinical and molecular aspects of neurotropic viral infections*. Gilden DH, Lipton HL (eds). Kluwer Academic Publishers: Boston, MA, pp 101–139.
- Lee VM-Y, Page CD, Wu HL, Schlaepfer WW (1984). Monoclonal antibodies to gel excised glial filament protein and their reactivities with other intermediate filament proteins. *J Neurochem* **42**: 25.
- Majno G, Joris I (1995). Apoptosis, oncosis, and necrosis. An overview of cell death. *Am J Pathol* **146**: 3–15.
- Navas S, Seo S, Chua MM, Das Sarma J, Lavi E, Hingley ST, Weiss SR (2001). The spike protein of murine coronavirus determines the ability of the virus to replicate in the liver and cause hepatitis. *J Virol* **75**: 2452–2457.
- Okuda Y, Bernard CC, Fujimura H, Yanagihara T, Sakoda S (1998). Fas has a crucial role in the progression of experimental autoimmune encephalomyelitis. *Mol Immunol* **35**: 317–326.
- Osborne BA (1996). Apoptosis and the maintenance of homeostasis in the immune system. *Curr Opin Immunol* **8**: 245–254.
- Palma JP, Yauch RL, Lang S, Kim BS (1999). Potential role of CD4+ T cell-mediated apoptosis of activated astrocytes in Theiler's virus-induced demyelination. *J Immunol* **162**: 6543–6551.
- Parra B, Lin MT, Stohlman SA, Bergmann CC, Atkinson R, Hinton DR (2000). Contributions of fas-Fas ligand inter- actions to the pathogenesis of mouse hepatitis virus in the central nervous system. *J Virol* **74**: 2447–2450.
- Razvi ES, Welsh RM (1995). Apoptosis in viral infections. *Adv Virus Res* **45**: 1–60.
- Sabelko KA, Kelly KA, Nahm MH, Cross AH, Russell JH (1997). Fas and Fas ligand enhance the pathogenesis of experimental allergic encephalomyelitis, but are not essential for immune privilege in the central nervous system. *J Immunol* **159**: 3096–3099.
- Shibata S, Kyuwa S, Lee SK, Toyoda Y, Goto N (1994). Apoptosis induced in mouse hepatitis virus-infected cells by a virus-specific CD8+ cytotoxic T-lymphocyte clone. *J Virol* **68**: 7540–7545.
- Tsunoda I, Fujinami RS (1996). Two models for multiple sclerosis: Experimental allergic encephalomyelitis and Theiler's murine encephalomyelitis virus. *J Neuropathol Exp Neurol* **55**: 673–686.
- Tsunoda I, Kurtz CI, Fujinami RS (1997). Apoptosis in acute and chronic central nervous system disease induced by Theiler's murine encephalomyelitis virus. *Virology* **228**: 388–393.
- Waldner H, Sobel RA, Howard E, Kuchroo VK (1997). Fas- and FasL-deficient mice are resistant to induction of autoimmune encephalomyelitis. *J Immunol* **159**: 3100–3103.
- Wu GF, Perlman S (1999). Macrophage infiltration, but not apoptosis, is correlated with immune-mediated demyelination following murine infection with a neurotropic coronavirus. *J Virol* **73**: 8771–8780.
- Zipp F, Weller M, Calabresi PA, Frank JA, Bash CN, Dichgans J, McFarland HF, Martin R (1998). Increased serum levels of soluble CD95 (APO-1/Fas) in relapsing-remitting multiple sclerosis. *Ann Neurol* **43**: 116–120.